Seismic imaging of karst

G.-A. Tselentis, N. Piliouras
University of Patras Seismological Center, Rio 261 10 Greece

Abstract

Tomographic methods, after their successful application in medicine, have started recently to be applied in various geological problems. In the present work, we have developed a methodology to delineate karst within coastal aquifers in order to locate the most appropriate sites for constructing fresh water wells. A simultaneous iterative reconstruction technique has been developed and was complemented with an accurate ray-tracing method in order to obtain an accurate tomographic image of the karst. The technique was applied to a coastal aquifer in central Greece and revealed a low velocity zone within the limestone which was later verified by drilling to correspond to a well developed karst within the rock mass, discharging large quantities of fresh water into the sea.

1 Introduction

Tomographic methods after their successful application in nuclear medicine (e.g. Cormack [4], Gullberg [10]), have started recently to be applied in various geophysical problems. Seismic tomography has been used for a number of applications of different kinds. Among these we may mention mineral exploration in mines (Gustavsson et al [11]), fault detection in coal seams (Mason [21], Bodoky et al [2]), stress monitoring in coal mines (Kormendi et al [18]), cave detection (Vazquez et al [27]), dam investigation (Cottin et al [6]), oil recovery projects (Macrides et al [22]) and rock investigation in connection with disposal of nuclear fuel waste Wong et al [28], Ivansson [15], Peterson et al [23], Gustavsson et al [11], Cosma [5], and Hammarstom et al [12]).

The purpose of the present investigation is to apply a seismic imaging technique employing cross-gallery data to delineate the karst between two galleries in a limestone coastal aquifer in central Greece.

A classic geophysical tomography problem is to reconstruct a velocity profile for some portion of the earth that travel times agree with the measurement. In practice, this is done by solving a large, sparse, least

squares problem. Traditional, least-squares problems in geophysical tomography have been solved by row-action methods such as: the algebraic reconstruction technique (ART) (Tanabe [25], Censor [3]), the simultaneous iterative reconstruction technique (SIRT) of Gilbert (Gilbert [8], Dines & Lytle [7], Ivansson [14]), the singular value decomposition (SVD) of Golub & Reinch [9] (e.g. Kanasewich & Chiu [17], Bishop et al [1]), the conjugate gradient (CG) algorithm of Hestenes & Stiefel [13] (e.g. Scales [24]).

In the present research, an algorithm was developed based on the SIRT method, (Simultaneous Iterative Reconstruction Technique). The tomographic reconstruction algorithm was implemented by a fast and accurate dynamic ray-tracing method for heterogeneous media based on the works of Langan et al [20] and Lafond & Levander [19].

2. The geotomography problem

Tomography involves production of an image of a medium from data that are line integrals of the parameter to be imaged. One of the simple problems in geophysical tomography is the inversion of traveltimes to obtain a subsurface velocity structure. The datum for seismic tomographic imaging is the integral of the slowness along a specified path through the medium.

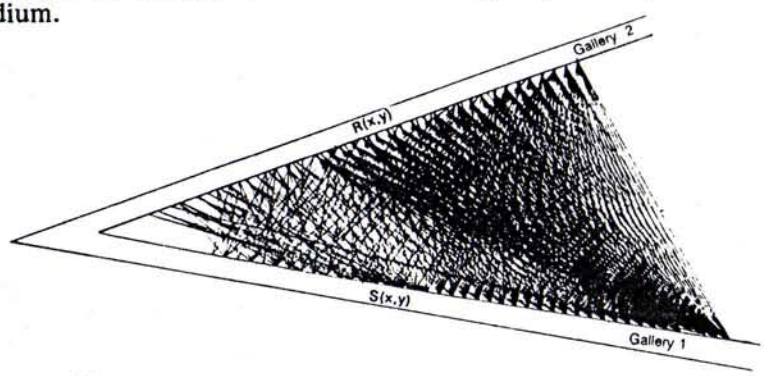

Fig 1: Typical cross-gallery seismic tomography arrangement (modified from Ivansson[16])

A typical simple two-dimensional source to receiver configuration involving galleries is depicted in Fig.l. Sources S(x,y) are excited sequentially in galleriy 1 and recorded on a string of recordeis R(x,y) in gallery 2. Each S is recorded at each R to provide a dense sampling of the medium between the galleries. The time spent by the seismic signal to travel from source to receiver along the ray is

$$t_{S,R} = L_{S,R}/V_{S,R} \qquad (1)$$

where $V_{S,R}$ is the mean velocity along the raypath $L_{S,R}$. By using $u_{S,R}$ as the slowness:

$$t_{S,R} = \frac{1}{V_{S,R}} \qquad (2)$$

we get

$$t_{S,R} = L_{S,R} u_{S,R}$$

The integral expression of eqn3 is

$$t_{S,R} = \int_{\Gamma} u(x,y)dL \qquad (4)$$

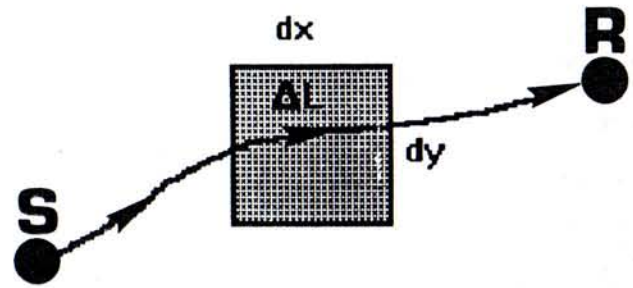

Fig 2: A ray in a 2-dimensional model.

By dividing the region to be imaged into a regular grid of cells and assigning a slowness u_{ij} in the (i,j) cell, the limit of eqn4 becomes

$$t_{S,R} = \sum_i \sum_j u_{ij} \ddot{A}L \qquad (5)$$

where ΔL (Fig.2) is the length of the intersection of the ray (S,R) with the cell (i,j).

A simple form for ΔL is

$$\Delta L^{i,j}_{S,R} = \frac{L_{S,R}}{K_{S,R}} \qquad (6)$$

where $L_{S,R}$ is the total length of a given ray and $K_{S,R}$ is the number of cells crossed by the ray. Eqn5 can be written

$$\frac{L_{S,R}}{K_{S,R}} \sum_i \sum_j u_{ij} h^{ij}_{S,R} \qquad (7)$$

where $h^{ij}_{S,R}$ is 1 if the ray (S,R) crosses the cell (i,j) and 0 otherwise.

A common practice is to use smoothed values instead of u_{ij}, allowing a certain contribution of the adjacent cells. The smoothing relations can facilitate the solution of the problem specially in the case of poor ray coverage and noisy data. The following smoothing expression is adopted

$$u_{ij} = (W-1)u_{ij} + \frac{\sum_{i-P}^{i+P}\sum_{j-r}^{j+r} u_{ij}N_{ij}}{\sum_{i-P}^{}\sum_{j-r}^{} N_{ij}} \tag{8}$$

where p and r give the extend of the smoothinη and W is the weight of the central cell. The, smoothing is weighted also by $N_{i,j}$, the number of rays crossing the adjacent cells. An initial guess u^o_{ij} is made for u_{ij} and prcnagation times are computed from eqn7. The differences between the measured and computed propagation times are found:

$$\Delta t^o_{S,R} = t_{S,R} - t^o_{S,R} \tag{9}$$

It is important to note that the error in apparent slowness is estimated for every ray by taking the average slowness for all rays crossing the same pixel

$$\ddot{A}u^0_{ij} = \frac{1}{N_{ij}}\sum_S \sum_R \frac{\ddot{A}t^0_{S,R}}{L_{S,R}} h^{i,j}_{S,R} \tag{10}$$

and the corrected slowness becomes

$$u^1_{ij} = u^0_{ij} + \Delta u^0_{ij} \tag{11}$$

the whole process is reiterated with the new values following the simultaneous iterative reconstruction technique- SIRT (Dines & Lyttle [7]).

3. Ray bending

So far data functionals used for the inversion procedure have been linearized by using fixed (straight) integration curves (see eqns 4&5). This may result in certain artifacts when the velocity structure is not homogeneous. The algorithm which we have developed considers realistic raypaths obeying Snell's low. We based our calculations on the kinematic raytracing procedure described by Langan at al [20] and the dynamic raytracing algorithm proposed by Lafond & Levander [19]. Starting with the raytracing system derived from the the eikonal equation

$$\frac{d}{dL}\left(u(r)\frac{dr}{dL}\right) = \left(u(r)\right) \tag{12}$$

where u(r) is the slowness at position r, L is the travel path length and integrating the above equation twice we obtain

$$r(L) = r_0 + n_0\int\frac{u(r_0)}{u(r)}dL' + \int\frac{1}{u(r')}\int V''u(r'')dL''dL' \tag{13}$$

where r_o and n_o are the position and direction of the ray at L=0. Defining a constant slowness gradient G as

$$G = \frac{V_r u(r)}{u(r)} \tag{14}$$

and integrating eqn13 approximately and keeping terms to the second order in G we obtain

$$r_i(L) = r_{0i} + n_{0i}\left[L + \frac{L^2}{2}(\mu_i - k) + \frac{L^3}{6}(3k^2 - G^2 - 2k\mu_i)\right] \tag{15}$$

with $k=G_i n_{oi}$, $\mu_i=G_i/n_{oi}$ and the index i running all over the three coordinates.

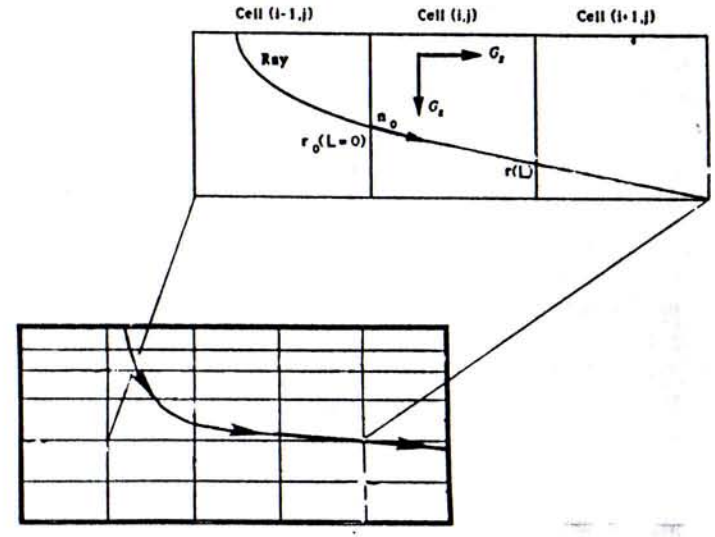

Fig 3: Ray bending geometry.

The direction n of the ray is obtained by differentiaing 15 with respect to the travel path L

$$n_i(L) = n_{0i}\left[1 + L(\mu_i - k) + \frac{L^2}{2}(3k^2 - G^2 - 2k\mu_i)\right] \quad (16)$$

and finally the travel time t(L) is obtained by integrating the product of the slowness and the ray direction along the travel path

$$t(L) = Lu_0\left[1 + \frac{Lk}{2} + \frac{L^2}{\beta}(G^2 - k^2)\right] \quad (17)$$

A simplified geometry of the raytracing is depicted in Fig.3. Following Lafond and Levander [19], for each cell we set the left hand side of eqnl5 to a position on one of the cell, boundaries and L is derived using Newon's method. Eqns 16 and 17 are used to compute the new ray direction and travel time and the process continues with the updated quantities for the next cell. Bicubic splines are used to interpolate between interfaces and Snell's law is used to assess the change of direction. A computer algorithm in turbo Pascal was written for the in-situ tomographic analysis of the collected data via a microcomputer (Tselentis and Piliuras [26]).

4. The field data

Data were collected at the Aluminum of Greece S.A. factory plant at Antikira (central Greece). The purpose of the field investigation was to delineate the geometry of the karst in the coastal limestone mass which consisted the only potential aquifer of the region. Since the rock mass of the limestone rock is relatively homogeneous and impermeable, the groundwater flow patterns are dominated by the major fracture zones and the karst. One major karstic zone was crossed during the construction of a gallery and resulted in considerable production rates. In order to delineate the geometry of the karst it was decided to perform a detailed tomographic investigation of the rock mass.

The first stage of the research initiated by contacting a detailed underground topographic mapping of the geometry of the galleries. Fig.4, depicts the geometry of the galleries and the source-receiver arrangement used. Data were collected using an ABEM Terraloc 24 channel signal enhancement digital seismograph. The seismic signals were generated by impacting with a hammer steel piles driven and cemented into the rock mass. First arrival times of seismograms were hand picked on a high-resolution graphics terminal. When more than one seismograms were available for the same source-receiver pair, the first arrival picks were averaged to give a single value. Twenty four geophones (digital grade wide band, natural frequency 10Hz, Sensor-Geosource) were locked along the sides of one gallery with cement at a spacing of 25 cm (Fig.5). Since the galleries were half filled with water, continuous pumping was necessary and was terminated only during recording times in order to improve signal to noise ratio.

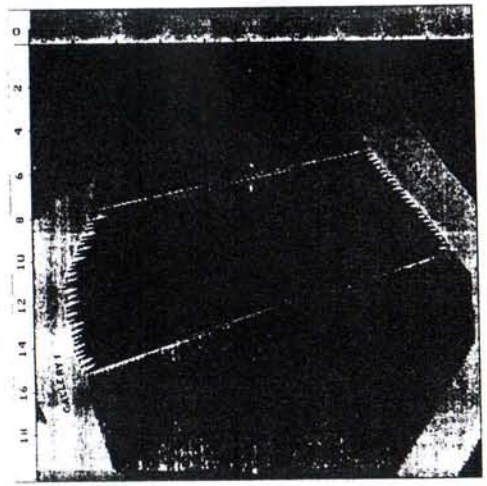

Fig 4: Geometry of the galleries and source-receiver arrangement.

The seismic measurements were performed at two levels, i.e. 0.2m and 1 m above the base of the galleries. Fig.6a,b depicts the results of the tomographic analysis at the two levels respectively. It is evident that the karst has been crossed by the first tomographic section while it is absent in the second section 1 m up, suggesting that its direction is from below upwards. Its position is towards the northwestern part of the section and this is in agreement with the results obtained from the exploratory drilling.

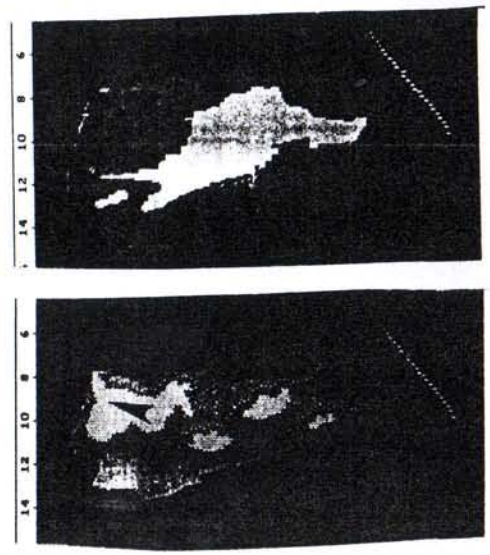

Fig 5: Results from the tomographic analysis. (a) Upper section, the light area is due to side reflections and does not correspond to karst. (b)Lower section, the karst is located towards the NW part.

Conclusions

In the present paper we developed a simultaneous iterative reconstruction technique complemented with an accurate ray-tracing method and we applied it for the seismic tomographic investigation of a karst in central Greece. The analysis of the collected data showed the geometry of the karst and pointed out the potential of seismic tomographic techniques in the solution of complicated geological problems.

Acknowledgments

The useful information and suggestions send by Dr. Nolet of the Dept. of Theoretical Geophysics of Utrecht University is acknowledged. We are also grateful to Drs. Lafond and Levander for sending details about their ray-tracing algorithm, and Dr. Ivansson for sending the details of Stripa Project. The research was founded by Aluminum of Greece SA and the useful contribution of the director of Environmental Engineering section Mr. Vgontzas and the engineer Mr. Nicolaidis are greatly appreciated.

References

1. Bishop, T., Bube, K., Cutler, R., Love, P., Resnick, J., Shuey, R., Spindler, D., and Wyld, H. Tomographic determination of velocity and depth in laterally varying media. Geophysics, 50, 903-923, 1985.

2. Bodoky, T., Hermann, L., and Dianiska, L. Processing of the in-seam seismic transmission measurements. 47th EAEG Meeting, Budapest, Hungary, 1985.

3. Censor, Y. Row action methods for huge and sparse systems and their applications. Soc. Industr. Appl. Math. Rev., 23, 444-466, 1981.

4. Cormak, A. Representation of a function by its line integrals, with some radiological applications. II, Appl. Phys., 34. 2772-2727, 1963.

5. Cosma, C. Crosshole investigations - short - and medium-range survey by seismic tomography, Stripa Project Internal report, SKBKBS, Stockholm, 1986.

6. Cottin, J-G., Deletie, P., Jacquet-Francillon, H., Lakshmanan, J., Lemoine, Y. and Sanchez, M. Curved ray seismic tomography: application to the Grand Etang dam (Reunion Island), First Break, 4:7, 25-30, 1986.

7. Dines, K., and Lytle, J. Computerized geophysical tomography. Proc. IEEE, 67,1065- 1073,1679, 1979.

8. Gilbert, J.F., 1972. Ranking and windowing gross Earth data for inversion and resolution. Geophys. J.R. astr. Soc., 43,125.

9. Golub, G.H., Van Loan C.F.,1983. Matrix computations. North Oxford Academic, Oxford.

10. Gullberg, G.,T., 1979. The attenuated Radon transform: theory and application in medical and biology. PhD thesis, Lawrence Berkeley Laboratory, University of California.

11. Gustavsson, M., Ivansson S., Moren, P., and Pihl, J.,1986. Seismic borehole tomographymeasurement system and field studies. Proc. IEEE, 74, 339-346.

12. Hammarstrom, M., Ivansson, S., Moren, P., and Pihl, J.,1986. Crosshole investigations - results from seismic borehole tomography, Stripa Project Internal Report, SKBKBS, Stockholm.

13. Hestenes, M.R., and Stiefel, E.,1952. Methods of conjugate gradients for solving linear systems. J. Res. N.B.S., 49, 409-436.

14. Ivansson, S., 1983. Remark on an earlier proposed iterative tomographic algorithm. Geophys. J. R. astr. Soc., 75, 855-860.

15. Ivansson, S.,1985. A study of methods for tomographic velocity estimation in the presence of low-velocity zones, Geophys, 50, 969-988.

16. Ivansson, S.,1987. Crosshole transmission tomography. In Seismic Tomography, Edit. G. Nolet.,159-189, Reidel Publ. Co.

17. Kanasewich, E.R.,1981. time sequence analyses in geophysics, The Univ. of Alberta Press.

18. Kormendi, A., Bodoky, T., Hermann, L., Dianiska, L.,, and kalman, T., 1986. Seismic measurements for safety in coal mines □ case histories, Geophys. prospecting, 34,122-132.

19. Lafond, C.F., and Levander, A.R., 1990 Fast and accurate dynamic raytracing in heterogeneous media. BuII. Seism. Soc. Am., 80,1284-1296.

20. Langan, R.T., Lerche, I., and Cutler, R.T., 1985. Tracing of rays through heterogeneous media: an accurate and efficient procedure, geophysics, 50, 1456-1465.

21. Mason, I.M., 1981. Algebraic reconstruction of α two-dimensional velocity inhomogeneity in the High Hazles seam of Thoresby colliery, Geophysics, 46, 298-308.

22. Macrides, C.G., Kanasewich, E.R., and Bharatha, S.,1988. Multiborehole seismic imaging in steam injection heavy oil recovery projects. Geophysics, 53,1, 65-75.

23. Peterson, J.E., Paulsson, B.N.P and McEvilly, T.V., 1985. Application of algebraic reconstruction techniques to crosshole seismic data, Geophysics, 50,1566-1580.

24. Scales, L.E.,1985. Introduction to nonlinear optimization, Mcmillan.

25. Tanabe, K.,1971. Projection method for solving a singular system of linear equations and its applications, Numer. math.,17, 203-214.

26. Tselentis G-A., and Piliuras, N.,1992. GEOSCAN: Aη algorithm for hard rock tomographic analysis. 2nd conference on Geotechnical Engineering, Thessaloniki, Oct. 21-23, Greece.

27. Vazquez, A., Aranda, R., and Benhumen, M.,1985. Cave detection using a tomographic algorithm, 47th EAEG Meeting, Budapest, Hungary.

28.Wong, J., Hurley, P., and West, G.F.,1985. Investigation of subsurface geological structure at the underground research laboratory with crosshole seismic scanning. Proceed. 17th information meeting of the Nuclear fuel Waste Management Program: TR-229, 593-608. Canada.